Clinical Biomechanics 29 (2014) 861–868

Contents lists available at ScienceDirect

Clinical Biomechanics

journal homepage: www.elsevier.com/locate/clinbiomech

Preclinical trial of a novel surface architecture for improved primary fixation of cementless orthopaedic implants

Noel Harrison [a], John R. Field [b], Fabio Quondamatteo [c], William Curtin [d], Peter E. McHugh [a], Pat Mc Donnell [a,*]

[a] Biomechanics Research Centre (BMEC), Biomedical Engineering, College of Engineering, National University of Ireland, Galway, Ireland
[b] Centre for Orthopaedic and Trauma Research (COTR), University of Adelaide, South Australia, Australia
[c] Skin and ECM Research Group, Anatomy, National University of Ireland, Galway, Ireland
[d] University College Hospital, Galway, Ireland

ARTICLE INFO

Article history:
Received 2 May 2014
Accepted 30 July 2014

Keywords:
Bone in-growth
Histology
Porous
Titanium
Stem
DMLS

ABSTRACT

Background: A new surface architecture for cementless orthopaedic implants (OsteoAnchor), which incorporates a multitude of tiny anchor features for enhancing primary fixation, was tested in an ovine hemi-arthroplasty pilot study.
Methods: Test animals were implanted with a hip stem component incorporating the OsteoAnchor surface architecture produced using additive layer manufacturing and control animals were implanted with stems containing a standard plasma sprayed titanium coating.
Findings: Intra-operative surgeon feedback indicated that superior primary fixation was achieved for the OsteoAnchor stems and rapid return to normal gait and load bearing was observed post-operation. Following a 16-week recovery time, histological evaluation of the excised femurs revealed in-growth of healthy bone into the porous structure of the OsteoAnchor stems. Bone in-growth was not achieved for the plasma sprayed stems.
Interpretation: These results indicate the potential for the OsteoAnchor surface architecture to enhance both the initial stability and long term lifetime of cementless orthopaedic implants.

1. Introduction

Total hip and knee replacement operations are routinely performed with generally successful outcomes. However, achieving good primary fixation, i.e. stability of the implant in the time period immediately after surgery, remains problematic for patients with poor bone stock. This is particularly the case in revision operations (Chung et al., 2012; Murphy and Rodriguez, 2004) where the patient's bone may already be osteoporotic and further bone damage can occur in removing the old implant. Although outcomes for implants with current surface coatings are generally very good, failure due to implant loosening does occur and a significant proportion of these are early failures after the initial operation (Melvin et al., 2014). Lack of good primary fixation can be a contributory factor in causing subsequent loosening and it has been shown that early migration of the stem after implantation is a predictor of subsequent implant loosening (Karrholm et al., 1994). It has also been reported that the effectiveness of the surface coating in providing early fixation influences the long term stabilisation of the stem (Callary et al., 2012). A new surface architecture for orthopaedic implants, OsteoAnchor (Harrison et al., 2013), has been developed at the authors' laboratory to improve primary fixation.

Long term stability of cementless orthopaedic implants requires effective primary fixation and secondary fixation to occur. Secondary fixation refers to the long term fixation of the implant, which is often achieved through bone in-growth into a porous coating on the implant (Valle et al., 2004). Effective primary fixation is required for successful secondary fixation to occur (Chang et al., 2011; Chanlalit et al., 2011; Gebert et al., 2009; Gotze et al., 2002; Sakai et al., 2006). If primary fixation is not achieved, excessive micromotions of the implant can result in the growth of fibrous tissue into the surface coating instead of hard bone (Cook et al., 1991; Soballe et al., 1992; Viceconti et al., 2001). This can lead to inadequate long term fixation of the implant. Loosening of the stem can subsequently occur and this may ultimately require revision surgery to be carried out. This problem is particularly relevant for patients with poor bone quality (Dayton and Incavo, 2005; Krischak et al., 2003).

Currently available surface coatings for cementless orthopaedic implants rely on press-fit and friction between the coating and the patient's bone to achieve primary fixation (Issa et al., 2014; Schiffern et al., 2005). It is therefore desirable that the surface coating exhibits a high coefficient of friction to enhance primary fixation and high porosity to facilitate substantial bone in-growth to provide long-term stable fixation of the implant. Sintered bead, plasma sprayed titanium, hydroxyapatite and wire mesh coatings have achieved very good clinical outcomes, but they possess relatively low porosity in the range of 30–50% and a low coefficient of friction (Levine and Fabi, 2010). More

* Corresponding author at: Biomechanics Research Centre (BMEC), College of Engineering and Informatics, NUI, Galway, Ireland.
E-mail address: pat.mcdonnell@nuigalway.ie (P. Mc Donnell).

http://dx.doi.org/10.1016/j.clinbiomech.2014.07.007
0268-0033/

recently, highly porous metal coatings have been developed (Benazzo et al., 2010; Bertollo et al., 2011; Bobyn et al., 1999; Frenkel et al., 2004; Meneghini et al., 2010) with higher porosity and coefficient of friction (Bourne et al., 2008; Gilmour et al., 2009; Levine and Fabi, 2010; Shirazi-Adl et al., 1993; Zhang et al., 1999). The OsteoAnchor surface architecture has been developed to further improve on the frictional properties of the currently available coatings, whilst maintaining a high porosity in the region of 64%. The surface architecture incorporates a multitude of tiny anchor features which are built onto a porous substructure in a one-step additive manufacturing process (Fig. 1). These anchor features are designed to reduce micromotions of the stem after implantation by embedding into the patient's bone and providing immediate mechanical fixation of the implant.

The objective of the current study was to test the primary fixation and bone in-growth performance of this new surface architecture in a load-bearing preclinical model. The hypothesis of the study was that the anchor features of the OsteoAnchor surface architecture would provide superior primary fixation compared to the plasma-sprayed control surface coating, and combined with the higher porosity substructure this would subsequently leadto more extensive secondary bone in-growth and implant stability.

2. Methods

An ovine hemi-arthroplasty model was chosen for this preclinical study and the work was carried out using skeletally mature merino sheep (Surgical Research Australia, Adelaide, Australia). The study incorporated a post-operative recovery period of 16 weeks. Since this was a pilot study to test the efficacy of the new surface architecture, animal numbers were kept low: three OsteoAnchor sheep and two control sheep completed the 16-week trial period. The study was approved by the Flinders University Animal Ethics Committee. At the end of the trial period, the sheep were sacrificed and the femurs were excised. Cross-sectional slices of the femur and implant were extracted and were prepared for histological analysis to evaluate the bone in-growth into the porous architecture.

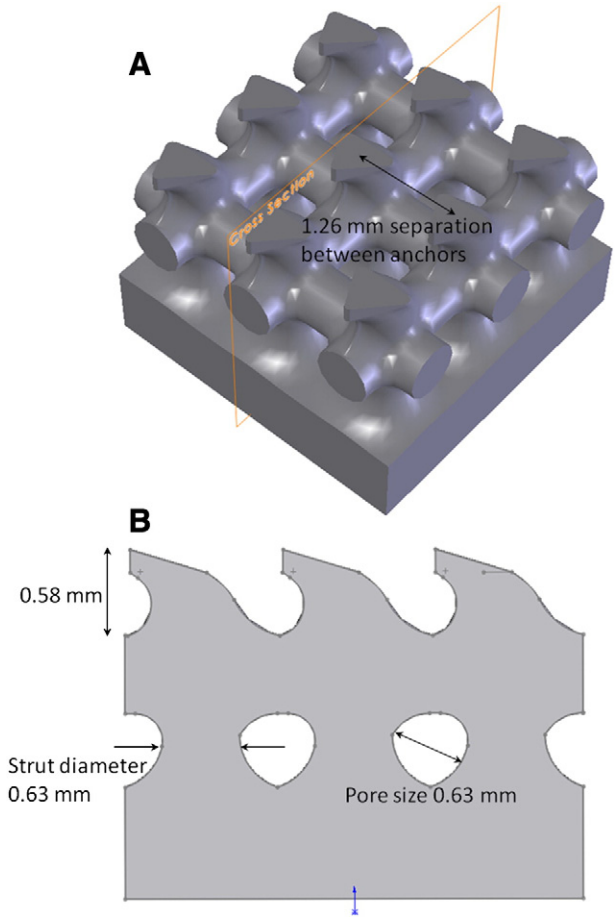

Fig. 1. OsteoAnchor surface architecture design.

2.1. Surface architecture and implant design

The detailed structure of the surface architecture for the OsteoAnchor stems was developed at the author's laboratory (National University of Ireland, Galway). The aim of this development process was to optimise the potential for primary fixation in the bone, ensuring sufficient strength to withstand in-vivo loading conditions and incorporating a highly porous lattice structure to enhance secondary bone in-growth. The final structure of the surface architecture that was developed incorporated a multitude of tiny anchor features on the bone-engaging side of the structure and an open-pore lattice beneath the anchor features to allow bone in-growth. The anchor features were specifically designed to embed into the bone during implantation, thus providing a secure fixation of the implant with the bone. A custom stem implant was developed which would incorporate the OsteoAnchor surface architecture and provide a press-fit in the trabecular bone of the metaphysis of the ovine femur. A number of design and prototyping iterations were required to optimise the stem geometry. Trial implantations were performed in excised ovine femurs to ensure that an adequate press-fit was achieved. The details of the final surface architecture and stem geometry design are given in the Results section.

2.2. Implant manufacture

The stems were manufactured using the direct metal laser sintering (DMLS) process (subcontracted to 3TRPD, Berkshire, UK using an EOS M270 DMLS system). The material used was Ti6Al4V. The OsteoAnchor surface architecture and the core geometry were built simultaneously to give a single, homogeneous part. Control implants were also manufactured with the same gross geometry as the OsteoAnchor stems, but with a separately applied plasma-sprayed porous coating of commercially pure (CP) titanium (Orchid Orthopaedic Solutions, Holt, MI, USA). The coating thickness for the control stems was 0.5 mm and had an average porosity of 30% or higher. This coating is representative of industry-standard plasma-sprayed cementless orthopaedic implants (Emerson et al., 2002; Mallory et al., 2001; Marshall et al., 2004).

Three different stem sizes were manufactured to allow the surgeon to intraoperatively select the stem which would give a good press-fit in individual animals. Standard 28 mm diameter, cobalt-chrome femoral head components were used (JRI Orthopaedics, Sheffield, UK), with a choice of three different neck length offsets. A custom surgical instrumentation set was designed and manufactured to facilitate broaching of the press-fit cavity in the metaphysis and consisted of a series of nine broaches of increasing size. The same instrumentation set was used during the operations for implanting the OsteoAnchor and control stems.

2.3. Surgery

Skeletally mature 3 to 4 year-old, castrated male Merino sheep (*Ovis aries*), bred for the purpose of research, were used in the study. Sheep were sourced from the Animal Facility, Flinders University, Melbourne, Australia. Sheep were a minimum of 50 kg in body weight with the mean and standard deviation of sheep weight between the OsteoAnchor and control groups closely matched (control group: 72.3 kg, standard deviation: 8.1 kg/OsteoAnchor group: 72.7 kg, standard deviation: 6.0 kg). A total of 8 sheep (hereafter referred to as NUIG 1–8) were used in the study. Due to the novelty of the press-fit implant design and associated instrumentation, optimisation of the

surgical procedure was required. During this phase of the project, three of the sheep were removed from the study before the 16 week trial period was completed due to surgery and recovery related issues. Once these issues were resolved, the remaining five sheep (three from the OsteoAnchor group and two from the control group) completed the 16-week trial duration.

Surgery was performed by an experienced veterinary surgeon at the facilities of COTR, School of Medicine (Flinders University, South Australia). Prior to surgery, anaesthesia was induced in the animals by intravenous administration of 20 mg/kg of thiopentone. A lateral curvilinear approach to the left hip was made. Pre-operative radiographic screening determined the appropriate size implant for each sheep. After neck resection, the proximal medullary canal was broached to accurately fit the stem and a modular prosthesis was pressed into place in neutral version. Cephalosporins (antimicrobials) were administered twice daily for three days post-operatively via indwelling jugular catheter (22 mg/kg). An ovine-specific analgesic agent, Xylazine, was administered via an indwelling jugular catheter continuously using a syringe driver (Sims-Graseby MS-26, Sussex, England, UK) at a dose of 1 mg/h. This also was continued for three days post-operatively.

The animals were housed in an acute recovery shed and restrained using a sling to allow hoof-touching weight bearing for three days post-operatively. Following this, animals were housed in small pens (3 m by 3 m) for 8 weeks, and were then held at pasture thereafter until the end of the study at 16 weeks. Water was provided ad libitum, and supplementary food (oaten and lucerne hay) was provided once daily.

Whilst in the acute recovery shed, animals were monitored 3 times daily. In the pens, and at pasture, animals were monitored daily. Radiographs were taken post-operatively and at 16 weeks post-operatively for both groups. The sheep were sedated using Detomidine (0.06 mg/kg i.m.) prior to the radiographic evaluation. Dual simultaneous exposures were obtained at 80–90 kV and 3–6 mA s depending on the size of the animal.

A validated seven point numeric locomotion scale ranging from 0 = normal locomotion to 6 = unable to stand or move was used to evaluate post-operative locomotion. Two observers familiar with sheep locomotion scored at each time-point the animals ambulating freely in their pens. The observer was blinded as to treatment. Locomotion was recorded as a score pre-operatively, at 6 weeks post-operatively and immediately prior to sacrifice at 16 weeks post-operatively.

Sheep were sacrificed with an intravenous administration of an overdose of barbiturate (pentobarbitone sodium, 9.75 g (30 ml) i.v.). Following sacrifice, the left femur of each sheep was explanted with minimal disturbance to the implanted stem and attached head to ensure that their integrity with the surrounding bone was undisturbed. The explanted femurs were stored at −18 °C and were transported to NUI Galway in this frozen condition where they were subsequently processed for radiography and histology analysis (Table 1).

2.4. Evaluation of excised femurs

The excised femurs were visually examined and were subjected to radiographic imaging analysis prior to sectioning for histology testing. Note that only the OsteoAnchor implants were sectioned for histology since it was found after necropsy that no bone attachment or ingrowth was achieved for the control stems. Radiographs were taken using a C-Arm in the anterior/posterior view and the medial/lateral view. The femurs with the implanted stems were then sectioned into segments of pre-set size which were used for cutting of histology slices. A custom designed cutting fixture was used to ensure that the location and orientation of the segments were consistent for all femurs.

Preparation of the segments for subsequent histological evaluation involved fixing in paraformaldehyde (PFA) solution, dehydration at one day intervals in increasing concentrations of ethanol (70%, 80%, 95% and 100%), and clearing in xylene. The segments were then embedded in epoxy and sectioned into slices of approximately 0.5 mm thickness using the slow speed diamond saw. In general, three slices were prepared from each segment. The slices were mounted on glass slides and ground/polished to approximately 250 μm thickness using a sequence of grinding papers (180, 340, 600, 800 followed by 4000 grit) on a bench-top rotating polisher. Staining was performed using Masson's trichrome stain and the slides were examined histologically.

Table 1
Summary of animals and implants used in the preclinical trial.

Sheep no.	Stem type	Femoral head details
NUIG 3	OsteoAnchor	28 mm head, short offset neck
NUIG 5	OsteoAnchor	28 mm head, large offset neck
NUIG 7	OsteoAnchor	28 mm head, small offset neck
NUIG 6	Control	28 mm head, medium offset neck
NUIG 8	Control	28 mm head, medium offset neck

3. Results

3.1. Surface architecture and implant development

The design and development process for the OsteoAnchor stems resulted in a novel surface architecture targeted at achieving optimum primary fixation and secondary fixation in the bone. It comprised an open-pore lattice created by a series of 0.63 mm diameter solid struts (Fig. 1). The pore size was approximately 0.63 mm × 0.63 mm × 1.26 mm deep. The solid struts followed the contours of the basic stem shape to maximise lattice strength. The mean porosity of the surface architecture was 63%. On the outermost aspect of the lattice, a series of anchors were positioned such that they embedded into the host bone during implantation. The anchors were oriented to resist subsidence, but not to impede removal of the implant. The anchors were spaced 1.26 mm apart and protruded up to 0.58 mm out from the main lattice structure. Each anchor was positioned at a junction of at least two lattice struts to maximise strength of the surface architecture. The outermost surface of the anchor was triangular in shape with the anchors being moderately sharp. The anchors protruded outward at an angle of approximately 15° to the main stem surface. The gross stem geometry that was developed consisted of a double-tapered short-stem implant located exclusively in the metaphysis of the femur with no distal stem component (Fig. 2). The total surface area available for bone in-growth of the small stem size option (size chosen by the surgeon during surgery for all sheep) was 910 mm^2. The stem incorporated a 12–14 taper-fit neck for connection and locking to the femoral head component.

3.2. Surgical procedure

Intra-operatively, it was found that implantation of the control stems in NUIG 6 and NUIG 8 was difficult. The surgeon rated the initial fixation of these control stems to be substantially inferior to the OsteoAnchor stems NUIG 3, NUIG 5 and NUIG 7. This was demonstrated by the OsteoAnchor stems being well seated with a good coverage of the femoral head by the acetabulum post-operatively. By contrast, it was difficult to achieve secure fixation of the control stems, with the result that cracking of the femur occurred, which required the use of 18-gauge cerclage wires to hold the stem in place.

3.3. Post-operation

Radiographic evaluation of the femurs immediately post-operation revealed that all stems were well positioned in the femur and good cover of the acetabulum was achieved (Fig. 3). The locomotion performance of the sheep receiving the OsteoAnchor stem was found to be superior to that of the sheep receiving the control stems over the 16-week trial period after the surgery (Table 2). Locomotion scoring, by

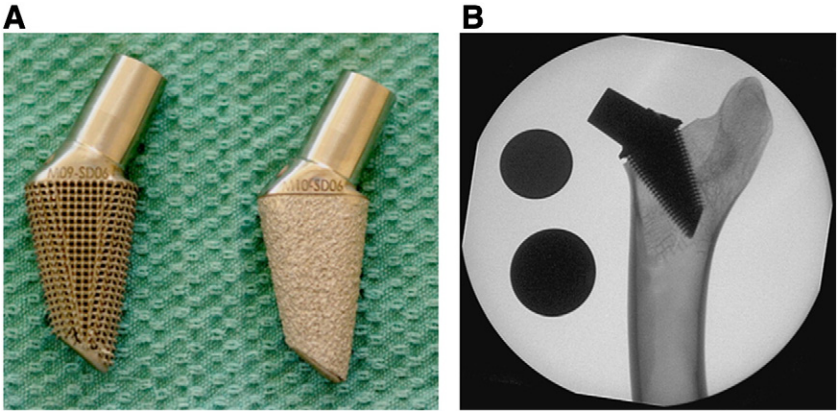

Fig. 2. Short-stem design for ovine hemiarthroplasty. A) Stem with test surface architecture (left) and control plasma-sprayed surface coating (right). B) Stem with test surface implanted in cadaver ovine femur.

two independent and blinded reviewers, indicated marginal lameness onset for the OsteoAnchor sheep during the immediate post-operative period. This improved to near-normal locomotion at 16 week recovery. By contrast, the control stem did not perform as well, with lameness still apparent after 16 week recovery.

3.4. 16 weeks post-operation

Following sacrifice of the animals at 16 weeks post-operation, radiographic evaluation of the femurs and implants was again carried out. It was found that control stem NUIG 6 had substantially subsided in the femur. For control NUIG 8, the femoral head had luxated from the acetabulum and the stem had dislocated completely from the femur. This had occurred sometime prior to the end of the trial period based on the amount of proliferative bone in evidence, particularly around the cranial aspect of the proximal femur. For the OsteoAnchor stems, the radiographs at 16 weeks post-operation showed that NUIG 3 had subsided in the femur. However, stems NUIG 5 and 7 remained well positioned without any subsidence. In addition, for NUIG 5 and 7, clear concentrations of bone growth were evident at specific locations around the stem (Fig. 3).

Necropsy was subsequently carried out and revealed that the overlying tissue response for the three OsteoAnchor implants appeared normal and wear on the acetabular cartilage was consistent for a hemiarthroplasty of this duration. The excised femurs showed some proliferative new bone around the proximal aspect of the stem.

For the control sheep NUIG 6, the acetabulum was found to be shallow and worn, suggestive of a mobile femoral head. A substantial amount of proliferative soft tissue surrounded the proximal femur primarily in response to the application of the cerclage wire. The stem itself was found to be loose in the femoral cavity and could be removed from the femur without any force once the cerclage wires had been taken out.

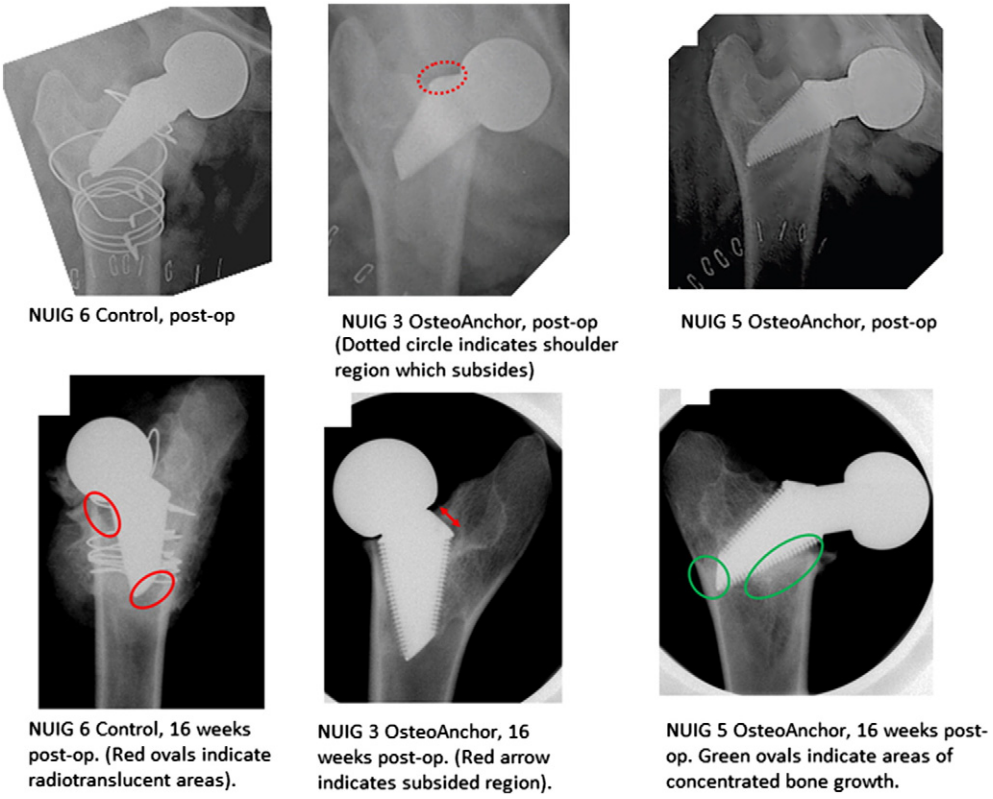

Fig. 3. Radiographic evaluation of implants and femurs, immediately post-op and 16 weeks post-op.

Table 2
Individual locomotion scores as assigned by two independent observers at the pre-operative, 6 and 16 weeks post-operative assessment times. A validated seven point numeric locomotion scale, ranging from 0 = normal locomotion to 6 = unable to stand or move, was used.

Sheep identification	Type of stem	Pre-operative	Post-operative (6 weeks)	Post-operative (16 weeks)
NUIG 3	OsteoAnchor	0, 0	1, 1	0, 1
NUIG 5	OsteoAnchor	0, 0	3, 3	1, 1
NUIG 7	OsteoAnchor	0, 0	3, 2	1, 1
NUIG 6	Control	0, 0	3, 3	2, 2
NUIG 8	Control	0, 0	3, 3	2, 2

Examination of the extracted stem showed that no bone in-growth had occurred into the plasma sprayed coating and there was also no fibrous tissue attachment. Similarly for control sheep NUIG 8, there was no bone in-growth or fibrous tissue attachment evident.

3.5. Histology evaluation

Histology evaluation was performed only on the OsteoAnchor femurs, since no bone in-growth was achieved in the plasma sprayed implants for the control femurs. The histology evaluation showed that for NUIG 3, the OsteoAnchor implant was surrounded by an annulus of fibrous tissue, which was in turn surrounded by an outer ring of cortical and trabecular bone. The fibrous tissue was directly attached to the implant surface and occupied the pores between the surface architecture struts.

Extensive bone in-growth was observed for NUIG 5 and almost the entire surface of the OsteoAnchor implant was directly in contact with bone tissue (Fig. 4). The struts of the surface architecture were fully surrounded by in-grown bone tissue and pores were also filled with bone tissue. Lamellar structures were observed in the bone, showing how the tissue had grown around the anchorsand struts and along the implant surface. Anterior, posterior, lateral and medial sides of the implant were fully surrounded by bone.

Bone in-growth was also observed for NUIG 7, particularly on the lateral end of the posterior surface (Fig. 5). There appeared to be little bone tissue in contact with the implant on the medial side of the implant. On the lateral posterior side, the implant was partially embedded into the cortical bone, with the cortical bone growing around the anchor features. On the lateral side, the implant was surrounded by and attached to trabecular bone.

The in-grown bone for NUIG 5 and 7 showed characteristic features that are typical of healthy bone. Lamellar structures were clearly visible (Fig. 6) containing lacunae, osteocytes, osteons and blood vessels. Clear attachment of the bone tissue to the Ti6Al4V implants was also apparent. A thin endosteal tissue was visible as a pink layer at the perimeter of most of the hard bone tissue volumes (i.e. between bone and marrow) and also lined the inside of the blood vessel canals.

4. Discussion

Inadequate primary fixation of cementless orthopaedic implants is considered to be an important contributor to loosening of implants in-vivo (Kroell et al., 2009). A new surface architecture, OsteoAnchor, which is manufactured as an integral part of the implant in a one step DMLS additive manufacturing process, has been developed to address this problem. An ovine hemi-arthroplasty model was chosen to test the effectiveness of this solution because, although it does not represent an osteoporotic model, it provides a challenging primary fixation application, i.e. there is limited trabecular bone quantity in the metaphysis of the femur and a short stem with a relatively small overall surface area was used to achieve press-fit and stability.

It was found that the OsteoAnchor implants provided superior primary fixation performance compared to the control plasma-sprayed titanium implants. This result is attributed to the mechanical interaction between the unique anchor features on the outer surface of the implants

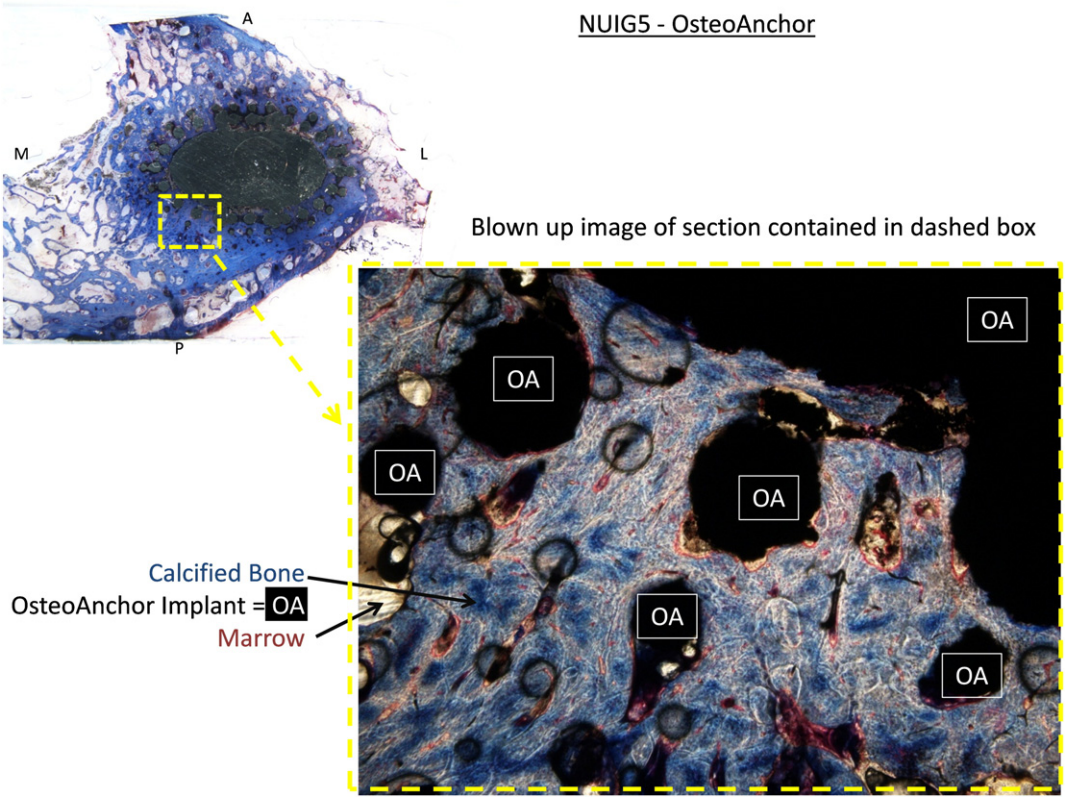

Fig. 4. Stereomicroscope image (top left) and zoom brightfield microscope image of a slide from segment 3 of NUIG 5, OsteoAnchor implant.

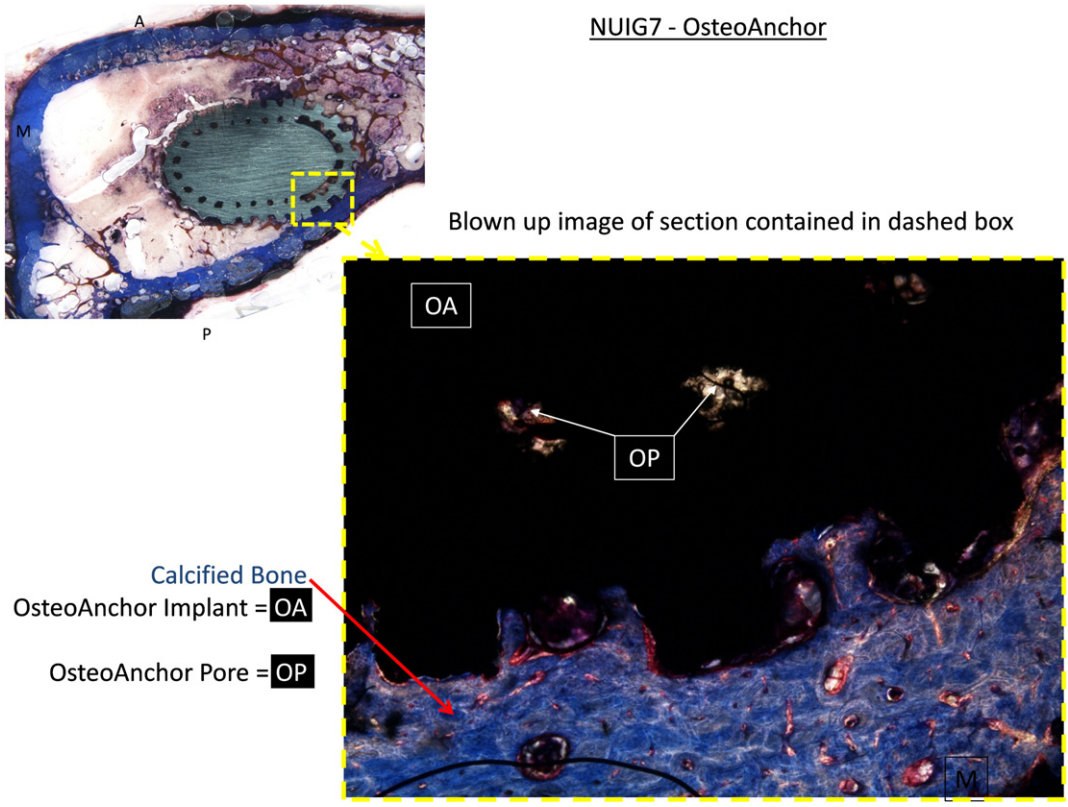

Fig. 5. Stereomicroscope image (top left) and zoom brightfield microscope image of a slide from segment 3 of NUIG 7, OsteoAnchor implant.

and the host bone. A prior bench testing study of the OsteoAnchor surface architecture demonstrated the effect of this mechanical interaction and showed that greater resistance to micromotion under physiological loading conditions was achieved compared to standard plasma sprayed and porous tantalum surface coatings that are currently in use (Harrison et al., 2013). For the control implants, it is likely that the initial difficulty

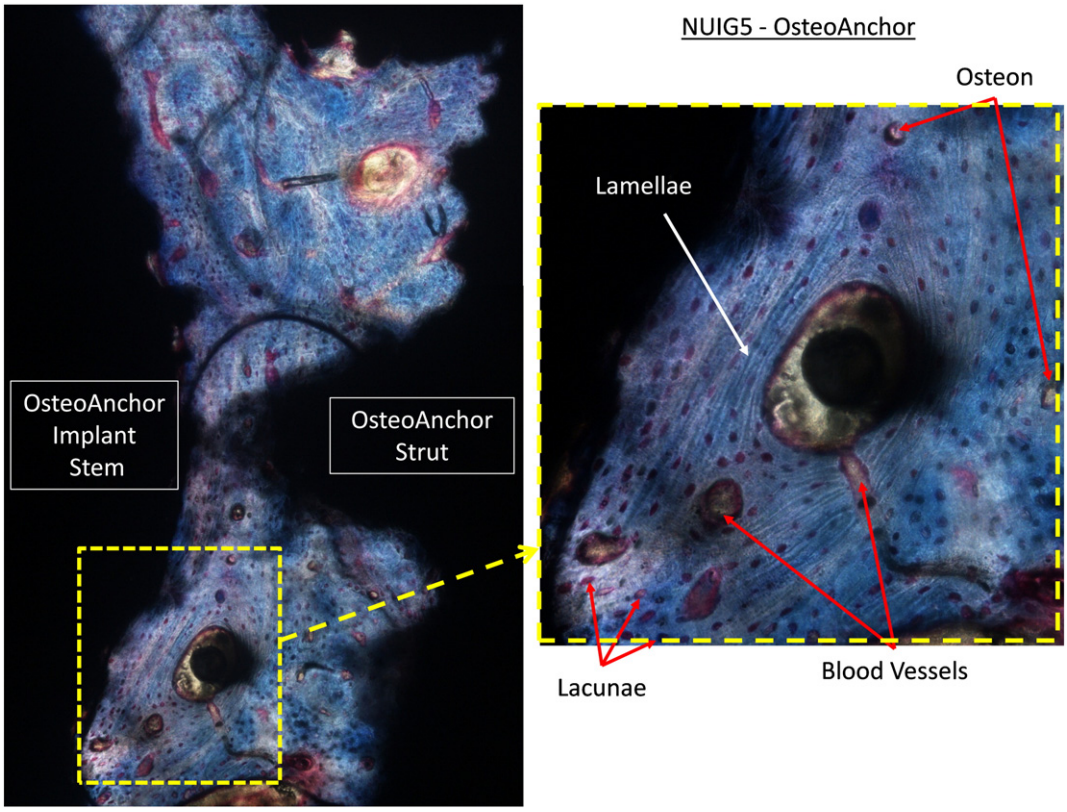

Fig. 6. In-grown bone structure, showing clear lamellae, lacunae and blood vessel structures.

in achieving primary fixation in this demanding short stem application was a major contributing factor to their failure to achieve any subsequent bone in-growth.

The OsteoAnchor implants were manufactured from Ti6Al4V alloy using the DMLS additive manufacturing process. There are no previous animal trial reports in the literature detailing the biocompatibility or otherwise of orthopaedic implants which are produced in this manner. The results of this study showed that there was no adverse tissue response to the DMLS produced implants, and in the case of the OsteoAnchor specimens, there was extensive bone in-growth into the porous structure and direct bone attachment onto the implant surface.

The post-operation trial duration of 16 weeks was a relatively short time period to allow extensive bone in-growth into the surface architecture, particularly for this type of load-bearing application. For the control stems, extension of the trial duration would most likely have made no difference to the level of bone in-growth. However, for the OsteoAnchor stems, it is possible that further development of bone in-growth would have been achieved for NUIG 5 if the trial duration had been longer. From the histology images for this specimen, it could be seen that trabecular bone structures were developing that had yet to ossify into hard bone. In addition, endosteal connective tissue was identified which contains osteoprogenitor cells that can differentiate into osteoblasts for bone growth and bone remodelling.

It should be emphasised that this was a pilot study to evaluate the potential for the OsteoAnchor surface architecture to provide improved primary fixation and subsequent bone in-growth. Therefore, due to ethical considerations, the number of animals included in the study was kept to a low number. Whilst statistical significance cannot be assigned to the results, the performance of the OsteoAnchor implants demonstrates the potential of the new surface architecture to address the primary stability problem. The conclusion is highlighted by the failure of the control implants to achieve any bone in-growth or attachment onto the plasma-sprayed surface coating. The choice of a plasma sprayed coating for the control stems of this study was based on the fact that this is a standard bone in-growth coating that has been successfully used on cementless orthopaedic implants for many years (Berend et al., 2004; Klein et al., 2006).

There are surprisingly few studies reported in the literature which have examined the primary fixation of implants in a load bearing preclinical model, given the fact that inadequate primary fixation is a major contributor to subsequent implant loosening. Press-fit stems have been used in preclinical trials to evaluate the effect of surface coatings on bone attachment (Carbone et al., 2006; Field et al., 2009; Howie et al., 2011; Ni et al., 2006; Yin et al., 2011). However, the effect of the surface coatings and treatments on primary fixation was not addressed in any of these studies. Stadelmann et al. evaluated the effect of local delivery of bisphosphonate from an implant on bone ingrowth using a sheep model (Stadelmann et al., 2009), with a view to combating the problem of poor primary fixation. However, they used small cylindrical implants inserted into the femoral condyle which were not subjected to the realistic physiological loading conditions on the stem components from this study. Elmengaard et al. adopted a similar approach to investigate the effect of Arg-Gly-Asp (RGD) peptide treatment of press-fit titanium implants by inserting cylindrical implants in the proximal tibia of mongrel dogs (Elmengaard et al., 2005). Although both of these studies showed that the selected surface treatment of implants improves bone in-growth and on-growth, the results could not be directly correlated with improved primary fixation, since the implants were not subjected to comparable loading regimes or the limited surface area for bone contact that is present for total joint replacements such as hip stems. By contrast, the surface architectures of the current study were tested on hip replacement stems which were subject to the physiological loading conditions and limited bone surface area contact which causes primary fixation problems in-vivo.

Conclusions

The results of this pre-clinical trial showed that the bone anchoring features of the OsteoAnchor surface architecture may facilitate superior primary fixation compared to a standard plasma sprayed surface coating. Although only three animals completed the 16-week trial duration with the OsteoAnchor stems, bone in-growth and attachment were achieved for the latter two of these implants, with extensive and almost full bone tissue filling of the porous substructure for NUIG 5. However, future work will be required to carry out additional preclinical trials to confirm the findings of the current pilot study. Specifically, an osteoporotic model is required for a follow on study, since this is more representative of the bone quality that exists in elderly osteoporotic patients. Nevertheless, the promising results of the study indicate the potential for OsteoAnchor to address orthopaedic clinical needs where primary fixation of the implant is difficult to achieve, for example in revision hip arthroplasty or augmentation applications.

Acknowledgements

The authors would like to acknowledge the support of Enterprise Ireland (grant number TD-2009-0143). This study was funded by Ireland's EU Structural Funds Programmes 2007–2013, co-funded by the Irish Government and the European Union. The contribution of Mark Canney (Anatomy Department, NUIG) and Muriel Voisin (Biomedical Engineering, NUIG) to the histology work is greatly appreciated. The authors would also like to acknowledge 3T RPD (Berkshire, UK) which manufactured the OsteoAnchor components using the DMLS process and EOS which provided expertise on optimisation of the DMLS process parameters.

References

Benazzo, F., Rossi, S.M.P., Piovani, L., Perticarini, L., Ghiara, M., 2010. Our experience with the use of TT (trabecular titanium) in hip arthroplasty surgery. J. Orthop. Traumatol. 11 (Suppl. 1), S53–S62.

Berend, K.R., Lombardi, A.V., Mallory, T.H., Dodds, K.L., Adams, J.B., 2004. Cementless double-tapered total hip arthroplasty in patients 75 years of age and older. J. Arthroplast. 19 (3), 288–295.

Bertollo, N., Matsubara, M., Shinoda, T., Chen, D., Kumar, M., Walsh, W.R., 2011. Effect of surgical fit on integration of cancellous bone and implant cortical bone shear strength for a porous titanium. J. Arthroplasty 26 (7), 1000–1007.

Bobyn, J.D., Stackpool, G.J., Hacking, S.A., Tanzer, M., Krygier, J.J., 1999. Characteristics of bone ingrowth and interface mechanics of a new porous tantalum biomaterial. J. Bone Joint Surg. 81b (5), 907–914.

Bourne, R.B., McCalden, R.W., Naudie, D., Charron, K.D., Yuan, X., Holdsworth, D.W., 2008. The next generation of acetabular shell design and bearing surfaces. Orthopedics 31 (12 Suppl), 12.

Callary, S.A., Campbell, D.G., Mercer, G.E., Nilsson, K.G., Field, J.R., 2012. The 6-year migration characteristics of a hydroxyapatite-coated femoral stem: a radiostereometric analysis study. J. Arthroplast. 27 (7), 1344–1348 (e1341).

Carbone, A., Howie, D.W., McGee, M., Field, J., Pearcy, M., Smith, N., Jones, E., 2006. Aging performance of a compliant layer bearing acetabular prosthesis in an ovine hip arthroplasty model. J. Arthroplast. 21 (6), 899–906.

Chang, J.-D., Kim, T.-Y., Rao, M.B., Lee, S-âS, Kim, I.-S., 2011. Revision total hip arthroplasty using a tapered, press-fit cementless revision stem in elderly patients. J. Arthroplasty 26 (7), 1045–1049.

Chanlalit, C., Fitzsimmons, J.S., Shukla, D.R., An, K.-N., O'Driscoll, S.W., 2011. Micromotion of plasma spray versus grit-blasted radial head prosthetic stem surfaces. J. Shoulder Elbow Surg. 20 (5), 717–722.

Chung, L., Wu, P., Chen, C., Chen, W., Chen, T., C. L., 2012. Extensively porous-coated stems for femoral revision: reliable choice for stem revision in Paprosky femoral. Orthopedics 35 (7), e1017–e1021.

Cook, S.D., Barrack, R.L., Thomas, K.A., Haddad Jr., R.J., 1991. Tissue growth into porous primary and revision femoral stems. J. Arthroplasty 6 (Supplement(0)), S37–S46.

Dayton, M.R., Incavo, S.J., 2005. Component loosening in total hip arthroplasty. Semin. Arthroplast. 16 (2), 161–170.

Elmengaard, B., Bechtold, J.E., Soballe, K., 2005. In vivo effects of RGD-coated titanium implants inserted in two bone-gap models. J. Biomed. Mater. Res. A 75 (2), 249–255.

Emerson Jr., R.H., Head, W.C., Emerson, C.B., Rosenfeldt, W., Higgins, L.L., 2002. A comparison of cemented and cementless titanium femoral components used for primary total hip arthroplasty: a radiographic and survivorship study. J. Arthroplast. 17 (5), 584–591.

Field, J.R., Stanley, R., Appleyard, R., McGee, M., Callary, S., Nilsson, K., 2009. An evaluation of prosthetic femoral head impact on acetabular articular cartilage in a hemiarthroplasty model. Vet. Comp. Orthop. Traumatol. 22, 142–147.

Frenkel, S.R., Jaffe, W.L., Dimaano, F., Lesaka, K., Hua, T., 2004. Bone response to a novel highly porous surface in a canine implantable chamber. J. Biomed. Mater. Res. B Appl. Biomater. 71 (2), 387–391.
Gebert, A., Peters, J., Bishop, N.E., Westphal, F., Morlock, M.M., 2009. Influence of press-fit parameters on the primary stability of uncemented femoral resurfacing implants. Med. Eng. Phys. 31 (1), 160–164.
Gilmour, L., Jones, B., Dickinson, J., 2009. Mechanical properties of a sintered asymmetric particle ingrowth coating. ASM Materials and Processes Conference 2009.
Gotze, C., Steens, W., Vieth, V., Poremba, C., Claes, L., Steinbeck, J., 2002. Primary stability in cementless femoral stems: custom-made versus conventional femoral prosthesis. Clin. Biomech. 17 (4), 267–273.
Harrison, N., McHugh, P.E., Curtin, W., Mc Donnell, P., 2013. Micromotion and friction evaluation of a novel surface architecture for improved primary fixation of cementless orthopaedic implants. J. Mech. Behav. Biomed. Mater. 21, 37–46.
Howie, D.W., McGee, M.A., Callary, S.A., Carbone, A., Stamenkov, R.B., Bruce, W.J., Findlay, D.M., 2011. A preclinical study of stem subsidence and graft incorporation after femoral impaction grafting using porous hydroxyapatite as a bone graft extender. J. Arthroplast. 26 (7), 1050–1056.
Issa, K., Pivec, R., Wuestemann, T., Tatevossian, T., Nevelos, J., Mont, M.A., 2014. Radiographic fit and fill analysis of a new second-generation proximally coated cementless stem compared to its predicate design. J. Arthroplast. 29 (1), 192–198.
Karrholm, J., Borssen, B., Lowenhielm, G., Snorrason, F., 1994. Does early micromotion of femoral stem prostheses matter? J. Bone Joint Surg. 76-B, 912–917.
Klein, G.R., Parvizi, J., Vegari, D.N., Rothman, R.H., Purtill, J.J., 2006. Total hip arthroplasty for acute femoral neck fractures using a cementless tapered femoral stem. J. Arthroplast. 21 (8), 1134–1140.
Krischak, G.D., Wachter, N.J., Zabel, T., Suger, G., Beck, A., Kinzl, L., Claes, L.E., Augat, P., 2003. Influence of preoperative mechanical bone quality and bone mineral density on aseptic loosening of total hip arthroplasty after seven years. Clin. Biomech. 18 (10), 916–923.
Kroell, A., Beaule, P., Krismer, M., Behensky, H., Stoeckl, B., Biedermann, R., 2009. Aseptic stem loosening in primary THA: migration analysis of cemented and cementless fixation. Int. Orthop. 33 (6), 1501–1505.
Levine, B.R., Fabi, D.W., 2010. Porous metals in orthopaedic applications — a review. Mat -wiss u Werkstoffech 41 (12), 1002–1010.
Mallory, T.H., Lombardi Jr., A.V., Leith, J.R., Fujita, H., Hartman, J.F., Capps, S.G., Kefauver, C.A., Adams, J.B., Vorys, G.C., 2001. Minimal 10-year results of a tapered cementless femoral component in total hip arthroplasty. J. Arthroplast. 16 (8, Supplement 1), 49–54.
Marshall, A.D., Mokris, J.G., Reitman, R.D., Dandar, A., Mauerhan, D.R., 2004. Cementless titanium tapered-wedge femoral stem: 10- to 15-year follow-up. J. Arthroplast. 19 (5), 546–552.
Melvin, J.S., Karthikeyan, T., Cope, R., Fehring, T.K., 2014. Early failures in total hip arthroplasty — a changing paradigm. J. Arthroplast. 29 (6), 1285–1288.
Meneghini, R.M., Ford, K.S., McCollough, C.H., Hanssen, A.D., Lewallen, D.G., 2010. Bone remodeling around porous metal cementless acetabular components. J. Arthroplasty 25 (5), 741–747.
Murphy, S.B., Rodriguez, J., 2004. Revision total hip arthroplasty with proximal bone loss. J. Arthroplast. 19 (4, Supplement 1), 115–119.
Ni, G.X., Chiu, K.Y., Lu, W.W., Wang, Y., Zhang, Y.G., Hao, L.B., Li, Z.Y., Lam, W.M., Lu, S.B., Luk, K.D., 2006. Strontium-containing hydroxyapatite bioactive bone cement in revision hip arthroplasty. Biomaterials 27 (24), 4348–4355.
Sakai, R., Kanai, N., Itoman, M., Mabuchi, K., 2006. Assessment of the fixation stiffness of some femoral stems of different designs. Clin. Biomech. 21 (4), 370–378.
Schiffern, S.C., Harrison, D.K., Burkhead Jr., W.Z., Krishnan, S.G., 2005. Cementless prosthetic fixation: when less is more—in the affirmative. Semin. Arthroplast. 16 (4), 257–262.
Shirazi-Adl, A., Dammak, M., Paiement, G., 1993. Experimental determination of friction characteristics at the trabecular bone/porous metal interface in cementless implants. J. Biomed. Mater. Res. 27, 167–175.
Soballe, K.S., Hansen, E.S., Rasmussen, H.B., Jorgensen, P.H., Bunger, C., 1992. Tissue ingrowth into titanium and hydroxyapatite-coated implants during stable and unstable mechanical conditions. J. Orthop. Res. 10 (2), 285–299.
Stadelmann, V.A., Terrier, A., Gauthier, O., Bouler, J.M., Pioletti, D.P., 2009. Prediction of bone density around orthopedic implants delivering bisphosphonate. J. Biomech. 42 (9), 1206–1211.
Valle, A.G., Zoppi, A., Peterson, M.G., Salvati, E.A., 2004. Clinical and radiographic results associated with a modern, cementless modular cup design in total hip arthroplasty. J. Bone Joint Surg. (Br.) 86-A (9), 1998–2004.
Viceconti, M., Monti, L., Muccini, R., Bernakiewicz, M., Toni, A., 2001. Even a thin layer of soft tissue may compromise the primary stability of cementless hip stems. Clin. Biomech. 16 (9), 765–775.
Yin, H., Li, J., Yu, X., Fu, Z., 2011. Effects of simvastatin on osseointegration in a canine total hip arthroplasty model: an experimental study. J. Arthroplast. 26 (8), 1534–1539.
Zhang, Y., Ahn, P.B., Fitzpatrick, D.C., Heiner, A.D., Poggie, R.A., Brown, T.D., 1999. Interfacial frictional behaviour: cancellous bone, cortical bone, and a novel porous tantalum biomaterial. J. Musculoskelet. Res. 3 (4), 245–251.